Arch. Metall. Mater. **65** (2020), 2, 621-626

DOI: 10.24425/amm.2020.132801

ENRIQUE ROCHA-RANGEL[1*], WILIAN J. PECH-RODRÍGUEZ[1], JUAN LÓPEZ-HERNÁNDEZ[1], CARLOS A. CALLES-ARRIAGA[1], EDDIE N. ARMENDÁRIZ-MIRELES[1], JOSÉ A. CASTILLO-ROBLES[1], JOSÉ A. RODRÍGUEZ-GARCÍA[1]

SYNTHESIS OF $SrTiO_3$ BY THE CALCINATION OF $SrCO_3$ AND TiO_2 MIXTURES INTENSIVELY GROUND BY MEANS OF HIGH ENERGY MILLING

A $SrTiO_3$ electroceramic with perovskite structure was produced by the calcination of a mixture of $SrCO_3$ and TiO_2 intensively grounded by high energy milling. For this purpose, raw materials were mixed in stoichiometric amounts in a planetary type mill; the obtained powder mixture was calcined for 2 h at temperatures between 800 and 1300°C. Samples resulting from the calcination were characterized by XRD, FTIR, SEM analysis and electrical measurements. From XRD, it was determined that the $SrTiO_3$ formed presents the cubic structure of perovskite. The complete reaction for $SrTiO_3$ compound formation occurs at 1200°C. Micrograph observations indicate the presence of a homogeneous microstructure with tiny grain size. The measured values of electrical resistivity were within the typical range of insulating materials.

Keywords: $SrTiO_3$, Mechanochemistry, Insulating ceramics, Perovskite

1. Introduction

Perovskite is a rare mineral in the earth's crust that crystallizes in cubic form. It is also the name of a crystals' group that has the same structure. Therefore, perovskites are cubic structures ceramics, which exhibit behavior from insulators to superconductors, passing through semiconductors, metallic conductors, manganites and ferroelectrics behaviors [1]. The alteration of the typical structure of the perovskites gives rise to the possibility of finding new electrical and magnetic properties, which makes interesting the study of materials with the perovskite structure.

Strontium titanate ($SrTiO_3$) is a compound of extraordinary importance in the field of electroceramics. At room temperature, it exists in the cubic perovskite form. It is considered a ferroelectric oxide because it presents high nonlinear optical coefficient, high dielectric constant, thermal stability and good photocatalysis [2]. In addition, it is characterized by having high mechanical strength, high thermal and chemical stability, low coefficient of thermal expansion and high melting temperature [3-4]. Due to all these properties, this compound has been used in a variety of applications such as thermistors [5], multilayer capacitors [6], electro-optical appliances [7], electromechanical devices [8], dynamic random-access memory [9] and field-effect transistors [10]. As every ceramic material, its final characteristics depend strongly on its microstructure and consequently by the processing route. Often the $SrTiO_3$ compound is processed by solid-state reactions between oxides such as SrO and TiO_2. This processing method implies work at high temperatures and long sintering times, which affect the microstructure considerably and thus electrical properties of the final compound [11-12]. There are many other methods to prepare the $SrTiO_3$, for example: sol-gel techniques [13-15], hydrothermal process [16-17], co-precipitation [18-19], microwave assisted [20], and combustion methods [21-23]. Although, these methods have advantages such as the control of the final chemical composition of the product, generally, they are costly, owing to the high costs of precursor reagents, jointly with the complexity of the experimental procedures, which makes them less productive methods. In the high-energy ball milling a powder mixture placed in a ball mill is subjected to high-energy collisions from the balls. High-energy ball milling, also called mechanochemistry or mechanical alloying, can successfully produce fine, uniform dispersions of a mixture of particles that cannot be made by conventional powder milling methods. So high-energy ball milling is a way of modifying the conditions in which chemical reactions usually take place, either by changing the reactivity of as-milled solids or by induc-

[1] UNIVERSIDAD POLITÉCNICA DE VICTORIA, AV. NUEVAS TECNOLOGÍAS 5902, PARQUE CIENTÍFICO Y TECNOLÓGICO DE TAMAULIPAS, CIUDAD VICTORIA, TAMAULIPAS, MÉXICO

* Corresponding author: erochar@upv.edu.mx

ing chemical reactions during milling. Due to these reasons the aim of this study is to manufacture the $SrTiO_3$ compound, by means of an intense grind by high energy of $SrCO_3$ and TiO_2 mixtures, combined with calcination at different temperatures and short times.

2.Experimental details

In this study, the $SrTiO_3$ compound was synthesized preparing mixtures in stoichiometric amounts according to reaction 1.

$$SrCO_3 + TiO_2 \rightarrow SrTiO_3 + CO_2\uparrow \quad (1)$$

2.1. Powder preparation and characterization

Powders of $SrCO_3$ and TiO_2 (Both; Sigma-Aldrich, 99.9% purity, and 1 mm size) were milled in a planetary type mill (Retsch PM 100, Germany) during 3 hours at a rotation speed of 300 rpm; a stainless steel container with zirconia grinding elements of 0.3 cm diameter was utilized. The powder weight – ball weight ratio was of 1:10. After milling, the particle size distribution and specific surface area were determined using a Mastersizer 2000 equipment of English origin. Observations of milled powders and microstructure of sintered samples were performed by scanning electron microscopy (JEOL, JSM 6300, Japan).

2.2. Solid-state reaction

The powder mixture resulting from the milling step was subjected to thermal treatments between 800 and 1300°C, in intervals of 100°C. This calcination was done in order to promote solid-state chemical reaction 1. The thermal treatment was carried out in an electric resistance furnace (Carbolite RHF17/3E, England) during 2 hours making an interval in each hour to grind the powder in a mortar and thus increase its surface area. The heating sped was 10°C/min. To determine the start and end temperatures of $SrCO_3$ decomposition, the pure unground powder of this compound was heated from room temperature and up to 1200°C in a thermogravimetric analysis unit (ADT/TG Shimadzu DTG-60, Japan).

2.3. Characterization of the calcined product

X-ray diffraction (XRD) and Fourier-transform infrared spectroscopy (FTIR) analyses were performed in (Siemens, D-5000, Germany) and (WQF-510A FTIR Rayleigh spectrometer instrument) devices respectively, to observe the progress of chemical reactions as a function of temperature for the formation of the $SrTiO_3$ perovskite. To carry out the FTIR analysis, the $SrTiO_3$ samples were mixed with KBr powder (Sigma-Aldrich, assay ≥99%), the obtained pellets were measured in transmission mode in a scan range of 4000-400 cm^{-1} at 4 cm^{-1} of resolution. These studies were done to determine the formation of the functional groups of the manufactured compound.

2.4. Electrical characterization

Measurements of resistivity and dielectric constant were performed at 0 Hz frequency (direct current) at room temperature, using the 4-point method, applying currents of the order of nanoamperes, through a controlled current source manufactured in our laboratories. This source was manufactured using circuits for stabilization of junctions in bipolar transistor [24]. This measurement was made only at 0 Hz, to have ample evidence of the electrical behavior of the manufactured material.

The resistivity was calculated in cylindrical samples according to equation 2.

$$\rho = \frac{d^2\pi}{4} \cdot \frac{V}{I} \cdot \frac{1}{L} \quad (2)$$

where: ρ stands for resistivity in units of (ΩM); d represents the diameter of the sample expressed in (mm); V is the potential difference shown in (V); I is the current intensity expressed in (A); and L is the thickness of the sample expressed in (mm).

3. Results and discussion

3.1. Powder grain size

The result of the particle size distribution analysis is reported in Fig. 1. In this figure it is observed the percentage of cumulative volume for the $SrCO_3$-TiO_2 powder mixture after the milling stage, in where it is perceived that approximately 50% of the powders have particle sizes under 10 micron; about 27% of particles present 10 to 50 microns in size; and the remaining

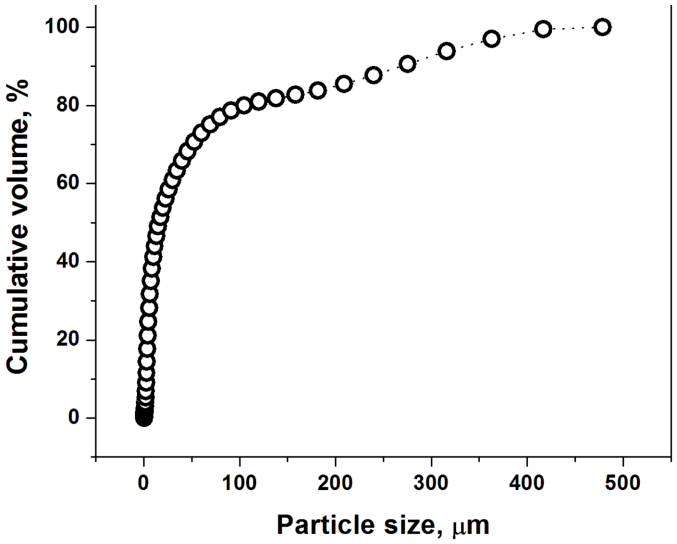

Fig. 1. Particle size distribution after intensively grounded by high energy milling

23% of powders are above 50 microns. The latter is probably due to the agglomeration of smaller powders. The specific surface area measured in the powder blend was 19.1 $m^2 \times g^{-1}$, this value suggests the existence of a large area of contact between the reactants ($SrCO_3$ and TiO_2) in order to complete the formation of the $SrTiO_3$ desired.

3.1.2. Powder morphology

Due to the high electrical resistance of ceramic compounds, on the order of MΩ, it was necessary to metalize the powder surface by depositing a gold-palladium film to obtain an improved resolution during the observation of its morphology by SEM. In the image of Fig. 2 are observed the morphology and size of the particles resulting from the milling stage. This figure shows the panoramic view of the powder at 5000 magnifications perceiving particles with a rounded shape, which is due to the used grinding method. Likewise, it is possible to appreciate that the size of these particles is well below 1 μm, which means, that we worked with very fine powders. The formation of agglomerates present in the image is due to having such fine powder sizes.

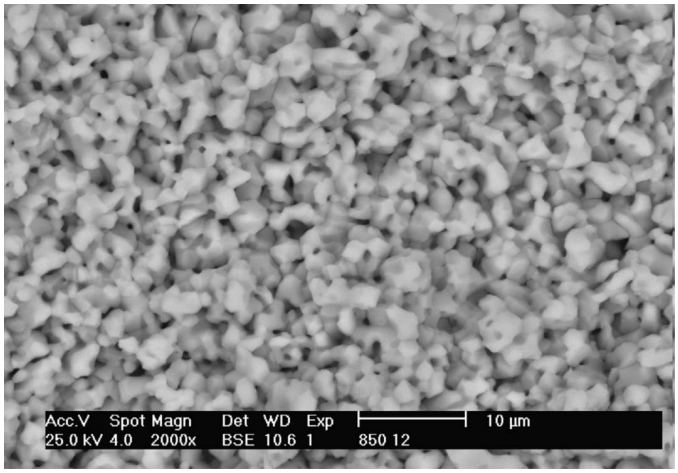

Fig. 2. Morphology of the particles resulting from the milling stage

3.2.Thermogravimetric analysis

Fig. 3 shows the result of the thermogravimetric analysis performed on pure unground $SrCO_3$. In this graph, it is observed that the beginning of the decomposition of $SrCO_3$ occurs at 750°C, whereas, the end of this decomposition occurs at 1,150°C. The total weight loss was 15% and corresponded to the release of CO_2 resulting from the decomposition of $SrCO_3$.

3.3. X-ray diffraction

X-ray powder diffraction technique was used to determine the progress of the reaction 1, as well as the crystal structure and phase of the compound. The parameters utilized were ac-

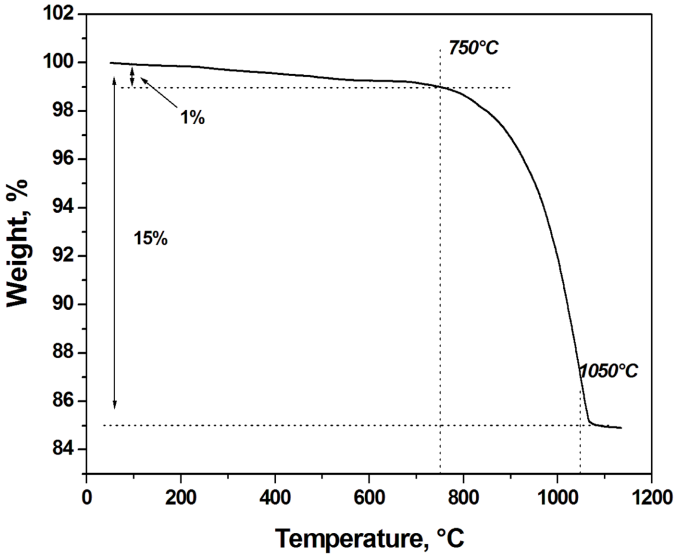

Fig. 3. Thermogravimetric analysis of pure unground $SrCO_3$

celeration voltage of 45 kV and current strength of 40 mA, with monochromatic copper line (Cu-α wavelength 1.540598 Å), with a step time of 2 °/min and a step size of 0.02° (2θ) in continuous mode, from 5° to 120° (2θ). The patterns obtained from the XRD study were analyzed aided by PANalytical X´Pert HighScore Plus software, to identify the phases of the compound by the intensities and the peaks of the graphs. Fig. 4 shows the XRD patterns obtained for samples calcined at different temperatures. In this figure, the most intense XRD peaks belong to the $SrTiO_3$ perovskite, while the peaks of lower intensity correspond to $SrCO_3$, which are precursor phase of perovskite. In the figure, it is observed that as the temperature increases, the corresponding peaks to $SrCO_3$ decrease in intensity, while the intensity of $SrTiO_3$ perovskite peaks increases. In the diffraction patterns corresponding to samples heat-treated at 1200 and 1300°C, all the peaks are indexed for cubic $SrTiO_3$. The lattice

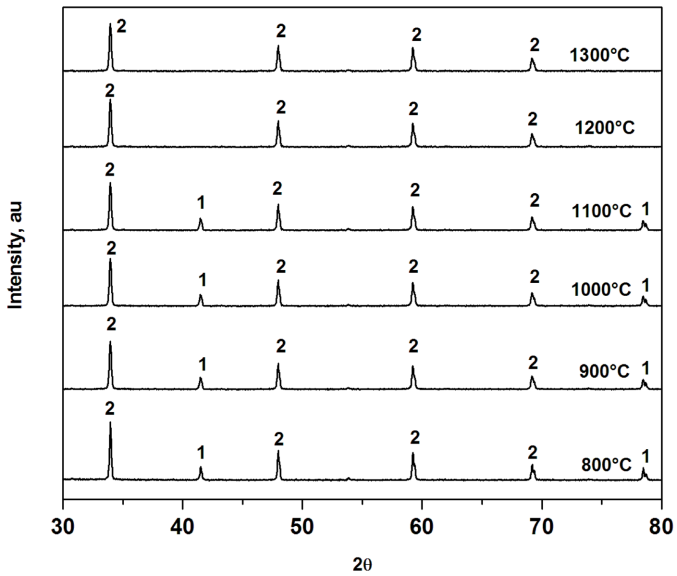

Fig. 4. XRD patterns of activated powders heat treated at different temperatures. 1: $SrCO_3$, 2: $SrTiO_3$

constant calculated from the XRD data is $a = b = c = 3.99$ Å, cell volume = 59.273 Å, and spatial group: Pm-3m, that agrees with the reported XRD data in JCPDS file (JCPDS 35-0734) for $SrTiO_3$. The original $SrCO_3$ and TiO_2 reactants are not observed above 1200°C. The lack of original compounds means that the formation reaction of $SrTiO_3$ is completed at this temperature. Considering the thermogravimetric curve of figure 3, the total decomposition of unground $SrCO_3$ occurs at 1,150°C. However, XRD results indicate that formation of $SrTiO_3$ perovskite by reaction 1 is completed at 1200°C. This formation means that the superficial activation and the good mixture of the reactant powders, due to the intensive grinding, favors the advance of the reaction 1, hence, at this low temperature of 1,200°C the desired product was already formed. Other studies have reported that $SrTiO_3$ formation generally occurs at temperatures above 1300°C [11-12].

The crystallite size for the resulting compound was calculated using the Debye-Scherrer Eq. (3) [25].

$$D = \frac{0.9_{k\alpha}}{B_{2\theta}\cos\theta} \tag{3}$$

where D represents the crystallite size, 0.9 is the shape factors for spherical particles, k the radiation wavelength (1.5406 Å), $B_{2\theta}$ is the full width at half maximum, and θ stands for the Bragg diffraction angle for the crystalline plane. The calculated value for the crystallite size was 50.1 nm. The initial materials have large crystallite size compared with the obtained $SrTiO_3$ compound suggesting that the solid state reaction contributed to the formation of pure $SrTiO_3$ nanoparticles at low temperatures.

3.4. Fourier-transform infrared spectroscopy (FTIR)

Fourier Transform Infrared Spectroscopy (FTIR) measurements were performed to identify the chemical bonds presented in the $SrTiO_3$ samples. Fig. 5 shows the FTIR spectrum of the synthetized $SrTiO_3$ samples. It can be observed an alteration band at 452 cm^{-1} due to Ti-O bonds vibrations [26-27]. Also, it can be noted a perturbation band located between 500-800 cm^{-1}, and it is ascribed to the stretching vibrations of $SrTiO_3$ [28]. Overall, the center of the last peak shift at high wavenumber as the treated temperature is increased. Meanwhile, the absorption band at 857 $cm^{-1}$and 1450 cm^{-1} are due to the presence of carbonate bonds CO-2 [29-30]. The peak around 1070 cm^{-1} is due to symmetric C-O stretching vibrations [31], and the perturbation at 1770 cm^{-1} is due to the C=O bond [32].

Fig. 6 displays the FTIR spectra of the $SrTiO_3$ samples in the range of 500-1000 cm^{-1}. As can be seen, the samples treated at 800 and 900°C present a peak of about 857 cm^{-1} that indicated the presence of carbonate. The samples treated at high temperatures do not reveal any peak at this wavenumber that indicated a complete formation of $SrTiO_3$. It is noteworthy to mention that the center peak shift at high wavenumber as the temperature increase, which suggest a bond strength increase.

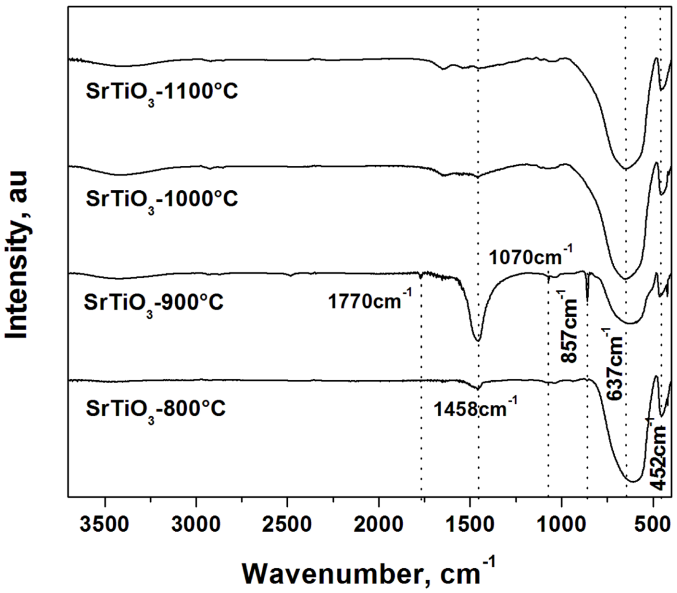

Fig. 5. FTIR spectra of the synthetized SrTiO3 samples at different temperatures

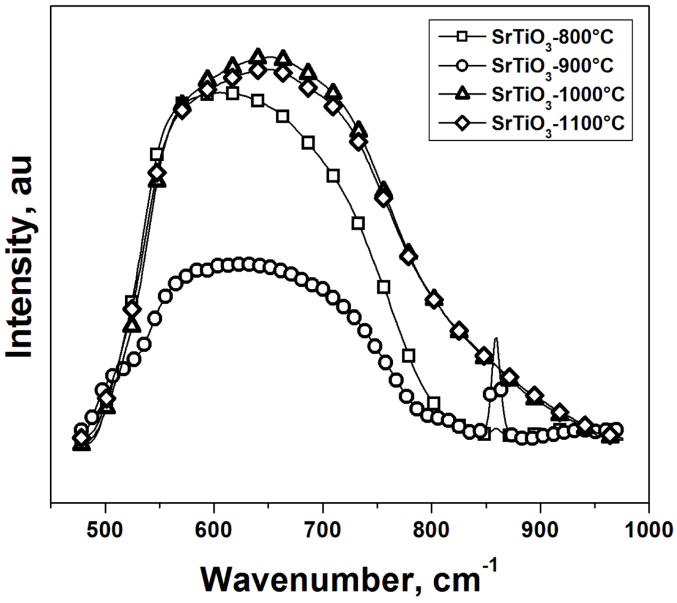

Fig. 6. FTIR spectra of the $SrTiO_3$ samples in the range of 500-1000 cm^{-1}

3.5. Microstructure

Fig. 7 shows an image of the microstructure of sample calcined at 1200°C during 2 h. It is noticed from this figure a microstructure with very small grains with round shapes; grain symmetries are due to the type of grinding process. The grain size ranges from several hundred nanometers to a few micrometers; this causes the formation of a large number of grain boundaries. These edges may favor high resistivity in the compound, since the passage of electrons through these areas is difficult, due to the high concentrations of energy that are held in them. On the other hand, it can be seen in the image that despite the very fine sizes of the powders there is no

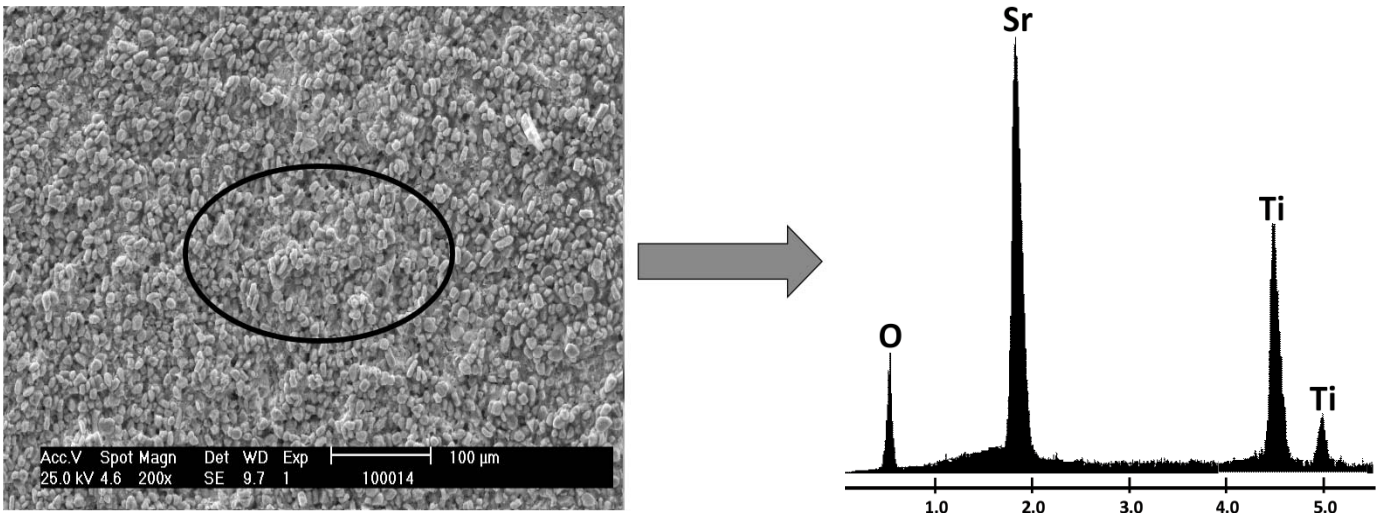

Fig. 7. Microstructure and EDS analysis carried out in the $SrTiO_3$ obtained

formation of large agglomerates of them. Figure 7 shows in a red circle the area considered to carry out an analysis by energy dispersive spectroscopy (EDS) aimed to find out the chemical elements present in the sample. In the EDS resulting spectrum, it is perceived the presence of Sr, Ti and O chemical elements that match up to the $SrTiO_3$ perovskite.

3.6. Electrical properties

Table 1 shows electrical properties, for instance, resistivity, conductivity and dielectric constant of calcined samples at different temperatures. In all cases resistivity´s values are upper than 1×10^{10} Wm; this means that the corresponding compound is within what it is considered as an insulating material. Alternatively, concerning the measurements of the dielectric constant shown in Table 1, it is observed a significant performance, due to the samples treated between 800 and 1,100°C present a very high dielectric constant. However, samples treated at 1200 and 1300°C exhibit a very small dielectric constant. This behavior can be explained in this way: in the samples treated below 1,100°C, reaction 1 is not complete. Therefore, the formation of the $SrTiO_3$ perovskite just has started, however, at these temperatures, there are still secondary phases such as SrO (this oxide results from the $SrCO_3$ decomposition) and TiO_2, that makes it hard for electrons to pass through the compounds. In agreement with FTIR and X-ray results at 1200 and 1300°C, reaction 1 was concluded, in this way the final compounds have the chemical composition and crystalline structure of the $SrTiO_3$ perovskite, exhibiting the characteristics of semiconductor material.

TABLE 1

Electrical properties measured in synthesized compounds as a temperature function

Synthesis temperature	Electric Conductivity	Electric resistivity	Dielectric constant
800°C	$3.21\times10^{-11}Sm^{-1}$	3.12×10^{10} Wm	696
900°C	$3.19\times10^{-11}Sm^{-1}$	3.14×10^{10} Wm	694
1000°C	$3.18\times10^{-11}Sm^{-1}$	3.14×10^{10} Wm	686
1100°C	$4.23\times10^{-11}Sm^{-1}$	2.36×10^{10} Wm	786
1200°C	$3.17\times10^{-11}Sm^{-1}$	3.15×10^{10} Wm	28
1300°C	$3.16\times10^{-11}Sm^{-1}$	3.16×10^{10} Wm	23

4. Conclusions

After promoting solid state reactions by means of an intense grind by high energy of $SrCO_3$ and TiO_2 mixtures and calcination, it was obtained pure $SrTiO_3$ perovskite-type with cubic structure at 1,200°C, as proved by XRD and FTIR analysis. SEM images showed the presence of very small grain sizes. Furthermore, the polymorphic shape of grains causes the formation of a large number of grain boundaries, which favors low values of resistivity in the obtained compound. Electrical measurements indicate that this kind of $SrTiO_3$ perovskites has very low electrical conductivity making them suitable for electronic applications, such as protector of electric shocks in electronic devices. In addition, the high dielectric constant and isolation capability presented by the $SrTiO_3$ compound make it suitable for capacitors miniaturization.

REFERENCES

[1] V.M. Fridkin, Photo-ferroelectrics, Springer, Berlin (1979).

[2] B. Maxim, Perovskites: Structure, Properties and Uses, Series: Chemical Engineering Methods and Technology, Nova Science Publishers, Hauppauge NY (2010).

[3] R.C. Neville, B. Hoeneisen, C.A. Mead, J. Appl. Phys. **43**, 2124-2131 (1972). https://doi.org/10.1063/1.1661463.

[4] M. Trainer, Am. J. Phys. **69**, 966-969 (2001). https://doi.org/10.1119/1.1374251.

[5] Y. Luo, X.Y. Liu, X.Q. Li, G.H. Chen. J. Alloy. Compd. **433**, 221-224 (2007). https://doi.org/10.1016/j.jallcom.2006.06.028

[6] M. Fujimoto, W.D. Kingery. J. Am. Ceram. Soc. **68**, 169-173 (1985). https://doi: 10.1111/j.1151-2916.1985.tb15292.x

[7] W. Kleemann, A. Albertini, M. Kuss, R. Lindner. Ferroelectrics. **203**, 57-74 (1997). https://doi:10.1080/00150199708012832

[8] Y.P. Guo, K. Kakimot, H. Ohsato, Solid State Commun. **129**, 279-284 (2004). https://doi.org/10.1016/j.ssc.2003.10.026

[9] Y. Watanabe, J.G. Bednorz, A. Bietsch, C. Gerber, D. Widmer, A. Beck, S.J. Wind, Appl. Phys. Lett. **78**, 3738-3740 (2001). https://doi.org/10.1063/1.1377617

[10] K Eisenbeiser. J.M. Finder, Z. Yu, J. Ramdani, J.A. Curles,s .JA. Hallmark, R. Droopad, W.J. OomsJ, L. Salem, S. Bradshaw, C.D. Overgaard, Appl. Phys. Lett. **76**, 1324-1326 (2000). http://hdl.handle.net/11455/11408

[11] L.C. Yan, J. Hassan, M. Hashim, W.S. Yin, T.F. Khoon, W.Y. Jeng, World Applied Sciences Journal. **14**, 1091-1094 (2011).

[12] L. Amaral L, A.M.R. Senos, P.M. Vilarinho, Mats. Res. Bull. **44**, 263-270 (2008). https://doi:10.1016/j.materresbull.2008.06.002

[13] H. Xu, S. Wei, H. Wang, M. Zhu, R. Yu, H. Yan, J. Cryst. Growth. **292**, 159-164 (2006). https://doi:10.1080/00150193.2013.848755

[14] W. Xuewen, Z. Zhiyong, Z. Shuixian, Mater. Sci. Eng. B. **86**, 29-33 (2001). https://doi.org/10.1080/00150193.2013.843412

[15] W.F. Zhang, Q. Xing, Y.B. Huang, Mod. Phys. Lett. B, **14**, 709-716 (2000). https://doi :10.1142/S0217984900000896

[16] S. Zhang, J. Liu, Y. Han, B. Chen, X. Li, Mater. Sci. Eng. B. **110**, 11-17 (2004). https://doi:10.1016/j.mseb.2004.01.017

[17] J. Jitputti, P. Charoensirithavorn, S.A. Yoshikawa, Chem. Lett. **36**, 1508-1509 (2007). https://doi.org/10.1246/cl.2007.1508

[18] P. Balaya, M. Ahrens, L. Kienle, J. Maier, B. Rahmati, S.B. Lee, W.A. Sigle, Pashkin, C. Kuntscher, M. Dressel, J. Am. Ceram. Soc. **89**, 2804-2811 (2006). http://hdl.handle.net/11858/00-001M-0000-0010-47F1-D

[19] P.K. Roy, J. Bera, Mater. Res. Bull. **40**, 599-604 (2005). https://doi.org/10.1016/j.materresbull.2005.01.010

[20] A. Shkabko, M.H. Aguirrea, I. Marozau, M. Doebeli, M. Mallepell, T. Lippert, A. Weidenkaff, Mats. Chem. Phy. **115**, 86-92 (2009). https://doi.org/10.1016/j.matchemphys.2008.11.024

[21] C.N. George, J. Thomas, R. Jose, H.P. Kumar, M.K. Suresh, V.R. Kumar, P.R. Shobana-Wariar, J. Koshy, J. Alloy. Compd. **486**, 711-715 (2009). https://doi.org/10.1016/j.jallcom.2009.07.045

[22] S. Liu, Z. Xiu, J. Liu, F. Xu, W. Yu, J. Yu, G. Feng, J. Alloys Compd. **457**, L12-L14 (2008). https://doi.org/10.1016/j.jallcom.2007.03.080

[23] H. Ishikawa, K. Oohira, T. Nakajima, T. Akiyama, J. Alloys Compd. **454**, 384-388 (2008). https://doi.org/10.1016/j.jallcom.2006.12.113

[24] B.L. Hart, The Radio and Electronic Engineer **50**, (1/2), 79-89 (1980).

[25] B.D. Cullity, S. R. Stock, Elements of X-Ray Diffraction, Prentice Hall, New Jersey (2001).

[26] N.T. Nolan, M.K. Seery, S.C. Pillai, J. Phy. Chem. C. **113**, 16151-16157 (2009). https://doi.org/10.1021/jp904358g

[27] T. Mahalingam, C. Selvakumar, K.E. Ranjith, T. Venkatachalam, Phys. Lett. A. **381**, 1815-1819 (2017). https://doi.org/10.1016/j.physleta.2017.02.053

[28] A.M. Youssef, H.K. Farag, A. El-Kheshen, F.F. Hammad, Silicon. **10**, 1225-1230 (2018). https://doi:10.1007/s12633-017-9596-z

[29] M.J. Kanaka, M. Ashutosh, B. Supriya, J. of Phy: Conference Series. **755**, 12-20 (2016).

[30] W.J. Pech-Rodríguez, C.A. Calles-Arriaga, D. González-Quijano, G. Vargas-Gutiérrez, C. Morais, T.W. Napporn, J. Power Sources. **375**, 335-344 (2018). http://dx-doi-org/10.1016/j.jpowsour.2017.07.081

[31] P.T. Tunç, F. Apaydin, K. Yildiz, J. Therm. Anal. Calorim. **127**, 63-69 (2017). https://doi.org/10.1007/s10973-016-5385-y

[32] F. Shi, P.N. Ross, G.A. Somorjai, K. Komvopoulos, J. Phy. Chem. C, **121**, 14476-14483 (2017). https://doi.org/10.1021/acs.jpcc.7b04132